ENHANCED PARTICLE TRACKING ALGORITHM BASED ON A MODIFIED EXPECTATION MAXIMIZATION ALGORITHM

Chad N. Young[1], David A. Johnson[2]

1: Department of Mechanical Engineering, University of Waterloo, Waterloo, ON, Canada, c2young@uwaterloo.ca
2: Department of Mechanical Engineering, University of Waterloo, Waterloo, ON, Canada, da3johns@uwaterloo.ca

Abstract An enhanced particle tracking algorithm is developed based on a modified expectation maximization algorithm. Particle tracking results using this method for a series of nine synthetic vortical test images are compared to results obtained using the algorithms of Baek & Lee and Labonte. The test cases utilized particle drop out, varying vortex sizes and shapes and other parameters to evaluate the algorithms. The appreciable improvement in the accuracy of EPTA tracking results for the test cases presented here shows the benefits of explicitly incorporating a vector field representation that is flexible yet regularized and serves as a model to both guide and constrain the process of determining particle correspondence. In particular, it is shown how two B-spline surfaces that are regularized using either a thin plate spline (TPS) or velocity-shear-dilation (VSD) model can accommodate flow gradients while attempting to maintain a degree of smoothness in the displacement field during the determination of particle-to-particle correspondence.

1. Introduction

Particle Tracking Velocimetry (PTV) algorithms are designed to track individual particles rather than particle clusters between temporally consecutive images. These algorithms are typically composed of three procedural steps in figure 1.

1. Identify individual particles and assign position indices

2. Track individual particles between images

3. Process tracking results
(e.g. Interpolation, spatial averaging and/or filtering)

Figure 1: Basic procedure for PTV

Step one is usually performed using a combination of image filtering procedures [14, 15], particle shape fitting [1, 17, 16, 5, 12], and/or image thresholding [6, 8, 11, 7, 4, 13]. Methods also exist by which occluding (i.e. overlapping) particle images can be separated [3]. Step two is the subject of discussion in this paper. Step three depends on experimental requirements and therefore is not considered further.

In principle, PTV algorithms can provide the highest possible spatial resolution because they allow for the identification and analysis the behaviour of individual particles. As such, they provide the potential to measure flow variations over the widest range of scales. Traditionally however, PTV approaches such as '*particle streak*' and '*nearest neighbours*' have been less popular compared to cross-correlation PIV due to particle number density limitations. In the same way that hierarchical implementations of conventional PIV algorithms developed over the last decade have led to improved spatial resolution, recent advancements to PTV algorithms have led to improved performance over a larger range of particle number densities and flow conditions.

A review of PTV techniques particularly the PTV algorithms developed by Baek & Lee [2, 13] and Labonte [10] were selected as benchmarks for comparison against the enhanced particle tracking algorithm (EPTA). The algorithms of Labonte and Baek & Lee represent important advancements in the field because they employ ideas akin to the idea of soft correspondence and thereby allow for the 'sharing' of correspondence information between neighbouring locales within an image. However, both methods are derived using models based on the assumption of parallel motion between neighbouring particles. As flow gradients increase and differences in displacement between neighbouring particles becomes larger, the validity of this assumption becomes increasingly questionable.

The EPTA incorporates a higher order displacement model that makes explicit allowance for flow gradients while at the same time attempting to maintain a degree of 'smoothness' in the displacement field. The EPTA utilizes a modified version of the expectation maximization algorithm that incorporates a regularized B-spline to represent the displacement field and the principle of Maxent to determine a set of particle correspondences between particles. As the algorithm iterates, the soft correspondences are slowly transformed into a set of hard correspondences that are used to determine the displacement of particles between image frames. Discussion is separated into two parts. In the first part, the utility of the EPTA algorithm is demonstrated in comparison with the algorithms of Baek & Lee [2, 13] and Labonte [10] using a series of synthetic test cases that contain periodic counter rotating vortices. The accuracy of EPTA tracking results shows the benefits of explicitly incorporating a flexible flow model that accommodates flow gradients and yet retains a sense of 'smoothness' between measured displacements obtained in neighbouring regions of an image. The concepts and ideas combined into the EPTA represent important advancements in the field of PTV that can allow for improved tracking performance over existing algorithms as flow gradients increase. However, there are issues with the EPTA that remain to be addressed before it can be considered robust enough for application over a wide range of PTV scenarios. In the absence of a reliable set of experimental data, synthetic flow profiles that contain periodic counter rotating vortices developed using equation 1 within a 256x256 pixel image were employed to test the utility of the EPTA. Each test case mimics the initial conditions of a Taylor-Green vortex field [9]. Idealized vortical structures are easily visualized and contain large gradients. Therefore they provide a good benchmark test of algorithm performance.

$$\Delta_x(x,y) = A\sin(\frac{2\pi x}{\omega_x})\sin(2\pi(0.25+\frac{y}{\omega_y}))$$
$$\Delta_y(x,y) = A\cos(\frac{2\pi x}{\omega_x})\cos(2\pi(0.25+\frac{y}{\omega_y})) \qquad (1)$$

In this equation the parameter A is the amplitude of the maximum measurable displacement and parameters ω_x and ω_y are used to control the size and shape of vortices in the image field. Values of A, ω_x and ω_y are specified in pixel units and are listed in table 1 for each of the nine test cases. Also listed in table 1 are other case identifying parameters including the number of vortices in the image, the nominal number of particles in the image, N_o, the displacement ratio, DR, and the displacement slope, DS. The displacement ratio, DR, is the ratio of the maximum particle displacement to the average distance between particles and is calculated as,

$$DR = \frac{A}{\sqrt{\frac{A_I}{\pi N_o}}} \qquad (2)$$

where A_I is the image area in pixels^2, and as above, A and N_o, are the maximum particle displacement and number of particles respectively. The displacement slope, DS, is a nominal average of the change in particle displacement over the span of a single pixel. It is calculated here

by dividing the maximum displacement by half of the dimension of a single vortex (i.e. 1/4 of the sinusoidal wavelength),

$$DS = \frac{4A}{\min(\omega_x, \omega_y)} \qquad (3)$$

The magnitudes of both DR and DS provide practical indications about the difficulty of the particle tracking problem. In general terms, the larger the magnitude of DR and/or DS the more difficult the particle tracking analysis becomes.

Nine synthetic test cases are used to benchmark the utility of the EPTA in comparison with the algorithms of Baek & Lee [2, 13] and Labonte [10]; however, it is important to note that this comparative analysis is not meant to *statistically quantify* the amount by which one algorithm is 'better' than another. Providing a conclusive comparison between the many existing PTV algorithms over a range of flow conditions has yet to appear in the literature and should be the subject of future work. With this in mind, it should also be noted that accomplishing such a task will not be a simple matter because there is not unified agreement about the important aspects that should make up such a comparison. These include:

1. the set of flow metrics and characterizing image parameters that should be used to classify and/or describe the broad spectrum of conditions in different PTV experiments,

2. the type of information that should be made available and/or used by a PTV algorithm prior to tracking (i.e. boundary conditions, more than two temporally successive images, particle shape and intensity information, etc.),

3. the criteria used to determine the effectiveness of a PTV algorithm and the range of metrics used to quantify the accuracy of tracking results, and

4. how results derived from comparative analyses should be applied when conducting a PTV experiment in cases where the flow field dynamics are not known a-priori.

Subject to the fact that these issues are unlikely to be resolved in the near future, a most effective approach to rationalize the application of one or more motion interrogation algorithms to a particular set of images is to understand the assumptions and comparative differences in operation between the various algorithms. Besides a thorough analysis of the theory supporting algorithm development, some of this understanding can be gleaned from the inspection of results obtained from benchmark tests.

Applying the EPTA

The methodology for applying the EPTA is shown in figures 2 and figures 3.

- The number of iterations, N_I, is computed in step D.2 by setting C_{N1} and C_{N2} to 1 and 5 respectively.

- The value of ε computed in step D.4 as a function of $C_{\varepsilon I}$ is computed by setting C_{knee} to the nominal value of 0.2.

- The B-spline patch size is initialized as 128x128 pixels and is reduced in a diadic fashion down to a minimum size of 32x32 pixels (i.e. C_{Hinit} = 1=2, $C_{Hreduct}$ = 2, and C_{Hmin} = 1/8). The value of *n* and ε_{thresh} used to compute the value of λ and the B-spline patch size at each

iteration, I, are set using the nominal values of 2 and 0.05 respectively.

- The value of the Lagrange multiplier, T, that controls the softness of the correspondences is initialized using, $C_{Tinit} = 3$, in step B.e, and is decremented in step D.6 using, $C_{TiterI} = 1 \quad \forall I$. The minimum value of T is set to the nominal value of 0.10 in step B.b.

- The null correspondence values computed in step D.1 are determined using $C_1 = 1$ and setting C_2 as shown in table 1.

With the exception of the parameter C_2, which is used to compute the null correspondence threshold, algorithm parameters remain the same for all test cases. The greater number of user defined parameters in the EPTA indicates the degree of flexibility afforded by the algorithm; however, greater flexibility can often mean more knowledge is required for effective algorithm application. With the EPTA this general rule is not allayed; however, the fact that only one user defined parameter is changed between test cases provides a measure of confidence about the ease with which the EPTA can be applied (at least to a certain class of similar flows).

Results

Algorithm Results for Test Cases

A summary of tracking results obtained by each algorithm for each of the nine test cases is shown in tables 2 and 3. In tables 2 and 3 the case parameters presented in the left-most columns are the same as in table 1 except for the additional columns denoting particle dropout percentage, and the actual number of particle correspondences, AC. The number of the figure corresponding to each case is also listed. Each test case is run five times to simulate different levels of particle dropout.

- In the first three of the five particle dropout scenarios, 0%, 10%, and 25% of the particles are removed from the image 1 and no particles are removed from image 2. Results from these '*few to many*' scenarios are shown in table 2.

- The last two particle dropout tests mirror the 10%, and 25% particle dropout tests above except that the time index is reversed. In this way the tracking of particles proceeds by analysing the motion of particles on image 2 as they move to indices on image 1. This simulates a '*many to few*' condition since there are more particles on the image 2 than on image 1. Results for these scenarios are shown in table 3.

Particle dropout cases are chosen to demonstrate the behaviour of the algorithm under controlled conditions as well as to represent endpoints on a continuum where particles are removed or added to both images. Summarizing metrics used to compare the tracking results for each of the algorithms are shown on the right of tables 2 and 3. These include:

- the number of measured correspondences, MC,
- the recovery ratio, RR = MC/AC,
- the number of correctly measured (valid) correspondences, VC,
- the measured error ratio, MER = VC/MC,
- and the total error ratio, TER = VC/AC,

A. Input: particle positions on images 1 and 2: $\{x_{1_i}, y_{1_i}\}, \{x_{2_j}, y_{2_j}\}$

B. Initialize:

a. $\overline{\varepsilon_{\min}} = 0.10$ b. $T_{\min} = \overline{\varepsilon_{\min}}$

c. $\underline{\theta}_{\mathrm{x}} = \underline{0},\ \underline{\theta}_{\mathrm{y}} = \underline{0},\ \mathbf{A} = \mathbf{0}$ d. $\sigma_x^2 = \sigma_y^2 = C_{\sigma^2} = 1$

e. $T = (C_{Tinit} \cdot R_{\max})^2,\ \ (1 \le C_{T_{init}} \le 4)$ f. $I = 1$

g. $C_{N1} = 1.5,\ \ (1.0 \le C_{N1} \le 2.5)$ h. $C_{N2} = 1.5,\ \ (5.0 \le C_{N2} \le 15)$

i. $C_1 = 1,\ \ (1.0 \le C_1 \le 3)$ j. $C_2 = 3,\ \ (1 \le C_2 \le 10)$

k. B-spline patch size quantities:

Initial patch size $= C_{Hinit} \cdot \min$ image dim $\ (1/8 \le C_{Hinit} \le 1)$

Minimum patch size $= C_{H\,\min} \cdot \min$ image dim $\ (1/32 \le C_{H\,\min} \le 1/4)$

Patch reduction parameter $= C_{Hreduct},\quad (C_{Hreduct} = 2)$

C. Compute: $\underline{\mathbf{\Delta}}_{\mathrm{x}}, \underline{\mathbf{\Delta}}_{\mathrm{y}}$

$$\{\Delta x_{ji}\} = \left\{x_{2_j} - x_{1_i}\right\}\ ,\quad \forall i,j\ ,\ \underline{\mathbf{\Delta}}_{\mathrm{x}} = lex\,\{\Delta x_{ji}\}$$

$$\{\Delta y_{ji}\} = \left\{y_{2_j} - y_{1_i}\right\}\ ,\quad \forall i,j\ ,\ \underline{\mathbf{\Delta}}_{\mathrm{x}} = lex\,\{\Delta y_{ji}\}$$

D. Loop $I = I + 1$

1. Compute: $\{\varepsilon_{ji}\}$

$$\varepsilon_{ji} = \frac{(\Delta x_{ji} - \mathbf{A}\underline{\theta}_{\mathrm{x}})^2}{\sigma_{\mathrm{x}}^2} + \frac{(\Delta y_{ji} - \mathbf{A}\underline{\theta}_{\mathrm{y}})^2}{\sigma_{\mathrm{y}}^2} \quad \forall i = 1 \text{ to } K,\ \forall j = 1 \text{ to } M$$

$$\varepsilon_{i,M+1} = \varepsilon_{K+1,j} = \max(C_1 \cdot T, C_2) \quad \forall i = 1 \text{ to } K,\ \forall j = 1 \text{ to } M$$

2. If $I = 1$ compute: $\{mask_{ji}\},\ N_I$

$$mask_{ji} = \begin{cases} 1 \text{ if } \varepsilon_{ji} \le R_{\max}^2 \\ 0 \text{ otherwise} \end{cases}$$

$$N_I = C_{N1} \cdot \frac{\sum_{i}^{K}\sum_{j}^{M} mask_{ji}}{\min(M,K)} + C_{N1} \cdot C_{N2}$$

3. Compute: $\{p_{ji}\}$

Initialize $p_{ji} = \exp(-\varepsilon_{ji}/T) \quad \forall i,j$

Figure 2: Enhanced particle tracking algorithm (EPTA) based on EM, continued in figure 3

4. Compute: $\overline{\varepsilon_1}$, $\overline{\varepsilon}$

$$\overline{\varepsilon_1} = \sum_i^K \sum_j^M p_{ij}\varepsilon_{ij} / \sum_i^K \sum_j^M p_{ij}, \text{ If } I = 1 \text{ set } \overline{\varepsilon}_{init} = \overline{\varepsilon_1}$$

$$\overline{\varepsilon} = C_{\varepsilon I} \cdot \overline{\varepsilon}_{init} + (1 - C_{\varepsilon I}) \cdot \overline{\varepsilon}_1$$

$$\overline{\varepsilon} = \overline{\varepsilon} - \left[\frac{\overline{\varepsilon} - \overline{\varepsilon}_{\min}}{(N_I - I) + 1} \right]$$

5. Compute: $\underline{\theta}_{\mathbf{x}}$, $\underline{\theta}_{\mathbf{y}}$, $\overline{\varepsilon_2}$, $Bsplinepatchsize$, λ

compute λ and B-spline coefficients, $\underline{\theta}_x$, $\underline{\theta}_y$

6. Redefine: $T = \left(\max(C_{TiterI} \cdot \overline{\varepsilon_2}, T_{\min})\right)^2$

Until

$$I > N_I$$

E. Freeze Solution:

1. $$p_{ji} = \left\{ \begin{array}{ll} 1 & \text{if } p_{ji} = \max\{p_{j1} \ldots p_{j,K+1}\}, \forall j \ \& \ p_{ji} = \max\{p_{1i} \ldots p_{M+1,i}\}, \forall i \\ 0 & \text{otherwise} \end{array} \right\}, \forall i = 1..K, \ j = 1..M$$

2. Compute: $\underline{\theta}_{\mathbf{x}}$, $\underline{\theta}_{\mathbf{y}}$

compute λ and B-spline coefficients, $\underline{\theta}_x$, $\underline{\theta}_y$

F. Return: $\{p_{ji}\}$, $\underline{\theta}_{\mathbf{x}}$, $\underline{\theta}_{\mathbf{y}}$

Figure 3: Enhanced particle tracking algorithm (EPTA) based on EM, continued from figure 2

Results are shown for the EPTA using both the thin plate spline (TPS) regularizer and the vorticity-shear-dilation (VSD) regularizer. As a guide to the reader, the relative improvement of the EPTA over the methods of Labonte [10] and Baek & Lee [2, 13] for each of these cases is most easily identified by comparing values of the TER (columns marked in bold).

General Observations from Tables 2 and 3

The results presented in tables 2 and 3 facilitate many comparative analyses however the following four general evaluations are the most important.

1. Except for case 1.1, both the thin plate spline (TPS) and vorticity-shear-dilation (VSD) versions of the enhanced particle tracking algorithm (EPTA) outperform the methods of Baek & Lee [2, 13] and Labonte [10]. For case 1.1, which is a single vortex with 200 particles, results for all methods are comparable. To quantify the improvement of the EPTA over the other methods, the average difference of the TER over all particle dropout scenarios is listed for each case in table 4. The most significant differences in the TER are observed for cases 3 through 9 where the combined effects of increased particle number density, greater particle displacement, and larger flow gradients make the tracking problem more difficult. Averaging TER values over all test cases, values obtained for the EPTA are higher than those of obtained for Labonte and Baek & Lee by 0.45 and 0.20 respectively.

2. Based on the results in tables 2 and 3 the differences between the TPS and VSD versions of

the EPTA are not large enough to make definitive conclusions about whether one method is superior to the other.

3. As a general rule, the best tracking results are obtained when there is no particle dropout. This observation is independent of the tracking algorithm employed. As particle drop out increases the tracking problem becomes more difficult for all of the algorithms. In general, the degradation of TER values from that obtained for the 0% particle dropout case is largest for the method of Labonte [10], but is also significant for the method of Baek & Lee [2, 13]. TER values are also degraded for the EPTA but to a lesser extent than for the other methods. Degradation of the TER for the EPTA is most evident only for the more complicated flows in cases 8 and 9 which contain 8 and 16 vortices respectively.

4. Except for the method of Labonte [10], the tracking results for all algorithms are better for the 'few to many' scenario than for the 'many to few' scenario. Over all test cases, the average difference between the TER value calculated for the 'few to many' and the 'many to few' scenarios are 0.11, 0.08, and 0.11, for the algorithm of Baek & Lee [2, 13] and the EPTA with TPS and VSD, respectively.

Results for one of the nine test cases is presented in figure 4 (case 2). In this figure, the plots across the top row depict particle indices and actual correspondences. Particles on image 1 are marked in blue and particles on image 2 are marked in red. Axes labels are in pixel units. Any particles encircled in green are those that appear on one image but do not appear on the other. The bottom four plots in each figure are the tracking results producing using each of the algorithms. Incorrectly tracked particles are encircled in magenta. Particles determined not to have a corresponding partner on the adjacent image are not shown. MER and TER values consistent with those in tables 2 and 3 are listed under each result.

Discussion of Figure 4

In the case of figure 4, where DR = 3.13 and DS = 0.125, the best tracking results are returned by the EPTA. By comparing the TPS and VSD versions of the EPTA, it is noted that the VSD provides slightly better performance in the corner regions where particle displacements are sharply reduced and the direction of motion changes rapidly. It is probably due to the fact that the 1st order VSD is a slightly less stringent smoothness model than the 2nd order TPS. The field results in figure 4 illustrate the improvement afforded by the EPTA in comparison with the other methods; however, it is also clear that there is still room for development. From analyses of iterate results (not shown) it appears that the tracking errors produced using the EPTA are linked to the way that the algorithm converges in each individual scenario. At present there does not exist a practical PTV algorithm that is general enough to be used in a variety of flows without significant user intervention and/or pretesting. As such, there still exist exciting opportunities for future research in the area of PTV and the future development of the EPTA and/or algorithms that employ ideas contained within the EPTA.

Conclusions

An enhanced particle tracking algorithm is developed based on a modified expectation maximization algorithm. The appreciable improvement in the accuracy of EPTA tracking results for the test cases presented here shows the benefits of explicitly incorporating a vector field representation that is flexible yet regularized and serves as a model to both guide and constrain the process of determining particle correspondence. In particular, it is shown how two B-spline

surfaces that are regularized using either a thin plate spline (TPS) or velocity-shear-dilation (VSD) model can accommodate flow gradients while attempting to maintain a degree of smoothness in the displacement field during the determination of particle-to-particle correspondence.

References

[1] R.J. Adrian and C-S Yao. Pulsed laser technique application to liquid and gaseous flows and the scattering power of seed materials. Applied Optics, 24(1):44–52, 1985.
[2] S.J. Baek and S.J. Lee. A new two-frame particle tracking algorithm using match probability. Experiments in Fluids, 22:23–32, 1996.
[3] F. Carosone, A. Cenedese, and G. Querzoli. Recognition of partially overlapped particle images using the kohonen neural network. Experiments in Fluids, 19:225–232, 1995.
[4] A. Cenedese and G. Querzoli. Lagrangian statistics and transilient matrix measurements by ptv in a convective boundary layer. Measurement Science and Technology, 8:1553–1561, 1997.
[5] E.A. Cowan and S.G. Monismith. A hybrid digital particle tracking velocimetry technique. Experiments in Fluids, 22:199–211, 1997.
[6] I. Grant and A. Liu. Directional ambiguity resolution in particle image velocimetry by pulse tagging. Experiments in Fluids, 10:71–76, 1990.
[7] Y.G. Guezennec and N. Kiritsis. Statistical investigation of errors in particle image velocimetry. Experiments in Fluids, 10:138–146, 1990.
[8] F. Hassan and T. Blanchet. Full-field bubbly flow velocity measurements by digital image pulsed velocimetry. Experiments in Fluids, 11:293–301, 1991.
[9] M. Ishikawa, Y. Murai, A. Wada, M. Iguchi, K. Okamoto, and F. Yamamoto. A novel algorithm for particle tracking velocimetry using the velocity gradient tensor. Experiments in Fluids, 29:519–531, 2000.
[10] G. Labonte. A new neural network for particle-tracking velocimetry. Experiments in Fluids, 26:340–346, 1999.
[11] H.G. Maas, A. Gruen, and D. Papantoniou. Particle tracking velocimetry in threedimensional flows – part 1. photogrammetric determination of particle coordinates. Experiments in Fluids, 15:133–146, 1993.
[12] M. Marxen, P.E. Sullivan, M.R. Loewen, and B. Jahne. Comparison of gaussian particle centre estimators and the achievable measurement density for particle tracking velocimetry. Experiments in Fluids, 29:145–153, 2000.
[13] K. Ohmi and H.-Y. Li. Particle tracking velocimetry with new algorithms. Measurement Science and Technology, 11:603–616, 2000.
[14] U.J. Schwartz. Mathematical-statistical description of the iterative beam removing technique (method clean). Astronomy and Astrophysics, 65:345–365, 1978.
[15] M. Stellmacher and K. Obernayer. A new particle tracking algorithm based on deterministic annealing and alternative distance measures. Experiments in Fluids, 28:506–518, 2000.
[16] DD. Udrea, P.J. Bryanston-Cross, W.K. Lee, and M. Funes-Gallanzi. Two sub-pixel processing algorithms for high accuracy particle centre estimation in low seeding density particle image velocimetry. Optics and Laser Technology, 28(5):389–396, 1996.
[17] M.P. Wernet and A. Pline. Particle displacement tracking technique and cramer-rao lower bound error in centroid estimates from ccd imagery. Experiments in Fluids, 15:295–307,1993.

Image Size: 256 x 256								Baek & Lee [2, 13] Parameters						Labonte [10] Parameters					EPTA Parameters								
Case	Figure	# Vortices	ω_x, ω_y	DR	DS	# Particles	Max. Disp.	r_A	r_B	R_{max}	R_n	t_E	N_I	R_{max}	R_o	R_f	α_o	N_I	R_{max}	C_{Hinit}	$C_{Hreduct}$	C_{Hmin}	C_{N1}	C_{N2}	C_{knee}	C_{Iter-I}	C_1	C_2
1	-	1	512, 512	1.56	0.125	200	16	0.3	4	17.6	28.78	3.19	25	17.6	128	2.6	0.01	25	17.6	0.5	2	0.125	1	5	0.2	1	1	9
2	-	1	512, 512	3.13	0.125	600	16	0.3	4	17.6	15.99	2.39	25	17.6	128	2.6	0.01	40	17.6	0.5	2	0.125	1	5	0.2	1	1	6
3	-	1	512, 512	2.71	0.25	200	32	0.3	4	35.1	25.53	7.98	25	35.1	128	2.6	0.01	25	35.1	0.5	2	0.125	1	5	0.2	1	1	9
4	-	1	512, 512	5.42	0.25	600	32	0.3	4	35.1	25.58	6.39	25	35.1	128	2.6	0.01	40	35.1	0.5	2	0.125	1	5	0.2	1	1	6
5	-	4	256, 256	1.36	0.25	200	16	0.3	4	17.6	25.47	7.16	25	17.6	128	2.6	0.01	25	17.6	0.5	2	0.125	1	5	0.2	1	1	9
6	-	4	256, 256	3.13	0.25	600	16	0.3	4	17.6	12.78	3.99	25	17.6	128	2.6	0.01	40	17.6	0.5	2	0.125	1	5	0.2	1	1	6
7	-	4	256, 256	2.71	0.5	200	32	0.3	4	35.1	25.43	11.12	25	35.1	128	2.6	0.01	25	35.1	0.5	2	0.125	1	5	0.2	1	1	9
8	-	8	256, 128	3.13	0.5	600	16	0.3	4	17.6	15.99	5.59	25	17.6	128	2.6	0.01	40	17.6	0.5	2	0.125	1	5	0.2	1	1	6
9	-	16	128, 128	3.13	0.5	600	16	0.3	4	17.6	12.79	7.20	25	17.6	128	2.6	0.01	40	17.6	0.5	2	0.125	1	5	0.2	1	1	6

Table 1: Parameters settings for test cases 1 through 9: Baek & Lee, Labonte, and EPTA.

Image Size: 256 x 256							Baek & Lee [2, 13]					Labonte [10]					EPTA: TPS					EPTA: VSD				
Case	Figure	# Vortices	# Particles	# Max Disp.	% Dropout	AC	MC	RR	VC	MER	TER	MC	RR	VC	MER	TER	MC	RR	VC	MER	TER	MC	RR	VC	MER	TER
1		1	200	16	0	200	195	0.975	195	*1.000*	**0.975**	200	1.000	200	*1.000*	**1.000**	199	0.995	199	*1.000*	**0.995**	199	0.995	199	*1.000*	**0.995**
					10	179	172	0.961	171	*0.994*	**0.955**	178	0.994	176	*0.989*	**0.983**	177	0.989	174	*0.983*	**0.972**	176	0.983	174	*0.989*	**0.972**
					25	149	140	0.94	138	*0.986*	**0.926**	147	0.987	141	*0.959*	**0.946**	145	0.973	138	*0.952*	**0.926**	147	0.987	138	*0.939*	**0.926**
2		1	600	16	0	599	580	0.968	568	*0.979*	**0.948**	480	0.801	347	*0.723*	**0.579**	592	0.988	586	*0.990*	**0.978**	598	0.998	598	*1.000*	**0.998**
					10	538	522	0.97	508	*0.973*	**0.944**	469	0.872	373	*0.795*	**0.693**	530	0.985	522	*0.985*	**0.970**	536	0.996	532	*0.992*	**0.989**
					25	448	434	0.969	416	*0.959*	**0.929**	379	0.846	229	*0.604*	**0.511**	422	0.942	404	*0.957*	**0.902**	424	0.946	403	*0.950*	**0.900**
3		1	200	32	0	199	176	0.884	164	*0.932*	**0.824**	197	0.990	195	*0.989*	**0.980**	193	0.970	188	*0.974*	**0.945**	198	0.995	198	*1.000*	**0.995**
					10	178	158	0.888	146	*0.924*	**0.820**	150	0.843	100	*0.667*	**0.562**	173	0.972	169	*0.977*	**0.949**	176	0.989	176	*1.000*	**0.989**
					25	149	128	0.859	120	*0.938*	**0.805**	128	0.859	96	*0.750*	**0.644**	145	0.973	139	*0.959*	**0.933**	141	0.946	137	*0.972*	**0.919**
4		1	600	32	0	600	499	0.832	413	*0.828*	**0.688**	403	0.672	196	*0.486*	**0.327**	586	0.977	577	*0.984*	**0.962**	596	0.993	592	*0.993*	**0.987**
					10	539	455	0.844	367	*0.807*	**0.681**	384	0.712	179	*0.466*	**0.332**	526	0.976	511	*0.971*	**0.948**	538	0.998	530	*0.985*	**0.983**
					25	449	375	0.835	284	*0.757*	**0.633**	290	0.646	85	*0.293*	**0.189**	444	0.989	422	*0.950*	**0.940**	447	0.996	433	*0.969*	**0.964**
5		4	200	16	0	200	185	0.925	178	*0.962*	**0.890**	195	0.975	190	*0.974*	**0.950**	199	0.995	199	*1.000*	**0.995**	199	0.995	199	*1.000*	**0.995**
					10	179	167	0.933	157	*0.940*	**0.877**	172	0.961	155	*0.901*	**0.866**	178	0.994	175	*0.983*	**0.978**	178	0.994	175	*0.983*	**0.978**
					25	149	133	0.893	119	*0.895*	**0.799**	135	0.906	118	*0.874*	**0.792**	142	0.953	135	*0.951*	**0.906**	143	0.960	139	*0.972*	**0.933**
6		4	600	16	0	599	547	0.913	523	*0.956*	**0.873**	433	0.723	255	*0.589*	**0.426**	594	0.992	594	*1.000*	**0.992**	598	0.998	598	*1.000*	**0.998**
					10	538	487	0.905	462	*0.949*	**0.859**	353	0.656	119	*0.337*	**0.221**	535	0.994	529	*0.989*	**0.983**	536	0.996	529	*0.989*	**0.983**
					25	448	396	0.884	360	*0.909*	**0.804**	321	0.717	99	*0.308*	**0.221**	439	0.980	419	*0.954*	**0.935**	436	0.973	421	*0.966*	**0.940**
7		4	200	32	0	200	136	0.680	80	*0.588*	**0.400**	116	0.580	8	*0.069*	**0.040**	199	0.995	199	*1.000*	**0.995**	198	0.990	197	*0.995*	**0.985**
					10	179	125	0.698	66	*0.528*	**0.369**	120	0.670	25	*0.208*	**0.140**	178	0.994	166	*0.933*	**0.927**	177	0.989	169	*0.955*	**0.944**
					25	149	107	0.718	59	*0.551*	**0.396**	101	0.678	27	*0.267*	**0.181**	134	0.899	96	*0.716*	**0.644**	140	0.940	97	*0.693*	**0.651**
8		8	600	16	0	597	460	0.771	358	*0.778*	**0.600**	340	0.57	63	*0.185*	**0.106**	581	0.973	559	*0.962*	**0.936**	582	0.975	559	*0.960*	**0.936**
					10	536	417	0.778	320	*0.767*	**0.597**	307	0.573	49	*0.160*	**0.091**	515	0.961	490	*0.951*	**0.914**	513	0.957	486	*0.947*	**0.907**
					25	446	353	0.791	248	*0.703*	**0.556**	304	0.682	58	*0.190*	**0.130**	407	0.913	296	*0.727*	**0.664**	419	0.939	337	*0.804*	**0.756**
9		16	600	16	0	596	378	0.634	238	*0.630*	**0.399**	354	0.594	55	*0.155*	**0.092**	577	0.968	561	*0.972*	**0.941**	575	0.965	553	*0.962*	**0.928**
					10	536	344	0.642	203	*0.59*	**0.379**	353	0.659	76	*0.215*	**0.142**	495	0.924	426	*0.861*	**0.795**	501	0.935	446	*0.890*	**0.832**
					25	446	300	0.673	172	*0.573*	**0.386**	301	0.675	66	*0.219*	**0.148**	419	0.939	347	*0.828*	**0.778**	419	0.939	354	*0.843*	**0.794**

Table 2: Comparison of tracking results for '**few to many**' scenarios with 0%, 10%, and 25% particle dropout. (AC = # Actual correspondences, MC = # Measured correspondences, RR = Recovery Ratio, VC = # of Valid Correspondences, MER = Measured error ratio, TER = Total error ratio.)

13th Int Symp on Applications of Laser Techniques to Fluid Mechanics
Lisbon, Portugal, 26-29 June, 2006
#1248

Image Size: 256 x 256							Baek & Lee [2, 13]					Labonte [10]					EPTA: TPS					EPTA: VSD				
Case	Figure	# Vortices	# Particles	Max. Disp.	% Dropout	*AC*	MC	RR	VC	MER	TER	MC	RR	VC	MER	TER	MC	RR	VC	MER	TER	MC	RR	VC	MER	TER
1	-	1	200	16	10	179	175	0.978	165	*0.943*	**0.922**	176	0.983	175	*0.994*	**0.978**	177	0.989	175	*0.989*	**0.978**	176	0.983	174	*0.989*	**0.972**
	-				25	149	145	0.973	127	*0.876*	**0.852**	146	0.980	141	*0.966*	**0.946**	145	0.973	140	*0.966*	**0.940**	140	0.94	135	*0.964*	**0.906**
2	-	1	600	16	10	538	526	0.978	495	*0.941*	**0.920**	461	0.857	351	*0.761*	**0.652**	536	0.996	529	*0.987*	**0.983**	534	0.993	529	*0.991*	**0.983**
	-				25	448	433	0.967	362	*0.836*	**0.808**	368	0.821	219	*0.595*	**0.489**	427	0.953	408	*0.956*	**0.911**	425	0.949	405	*0.953*	**0.904**
3	-	1	200	32	10	178	156	0.876	135	*0.865*	**0.758**	136	0.764	78	*0.574*	**0.438**	173	0.972	169	*0.977*	**0.949**	176	0.989	176	*1.000*	**0.989**
	-				25	149	133	0.893	108	*0.812*	**0.725**	137	0.919	110	*0.803*	**0.738**	144	0.966	142	*0.986*	**0.953**	141	0.946	137	*0.972*	**0.919**
4	-	1	600	32	10	539	449	0.833	345	*0.768*	**0.640**	349	0.648	70	*0.201*	**0.130**	527	0.978	507	*0.963*	**0.941**	533	0.989	522	*0.979*	**0.968**
	-				25	449	369	0.822	258	*0.699*	**0.575**	321	0.715	80	*0.250*	**0.178**	440	0.98	416	*0.946*	**0.927**	421	0.938	332	*0.789*	**0.739**
5	-	4	200	16	10	179	158	0.883	143	*0.905*	**0.799**	178	0.994	178	*1.000*	**0.994**	169	0.944	149	*0.882*	**0.832**	173	0.966	156	*0.901*	**0.872**
	-				25	149	135	0.906	102	*0.756*	**0.685**	131	0.879	100	*0.763*	**0.671**	138	0.926	119	*0.862*	**0.799**	141	0.946	126	*0.894*	**0.846**
6	-	4	600	16	10	538	475	0.883	408	*0.859*	**0.758**	365	0.678	128	*0.351*	**0.238**	536	0.996	529	*0.987*	**0.983**	524	0.974	495	*0.945*	**0.920**
	-				25	448	385	0.859	286	*0.743*	**0.638**	338	0.754	138	*0.408*	**0.308**	410	0.915	388	*0.946*	**0.866**	412	0.92	389	*0.944*	**0.868**
7	-	4	200	32	10	179	124	0.693	71	*0.573*	**0.397**	113	0.631	24	*0.212*	**0.134**	164	0.916	131	*0.799*	**0.732**	161	0.899	131	*0.814*	**0.732**
	-				25	149	108	0.725	50	*0.463*	**0.336**	105	0.705	32	*0.305*	**0.215**	142	0.953	85	*0.599*	**0.570**	141	0.946	82	*0.582*	**0.550**
8	-	8	600	16	10	536	421	0.785	288	*0.684*	**0.537**	342	0.638	79	*0.231*	**0.147**	476	0.888	369	*0.775*	**0.688**	470	0.877	366	*0.779*	**0.683**
	-				25	446	364	0.816	216	*0.593*	**0.484**	304	0.682	52	*0.171*	**0.117**	403	0.904	249	*0.618*	**0.558**	403	0.904	250	*0.620*	**0.561**
9	-	16	600	16	10	536	351	0.655	161	*0.459*	**0.300**	354	0.66	78	*0.220*	**0.146**	431	0.804	261	*0.606*	**0.487**	432	0.806	262	*0.606*	**0.489**
	-				25	446	308	0.691	120	*0.390*	**0.269**	314	0.704	50	*0.159*	**0.112**	374	0.839	232	*0.620*	**0.520**	376	0.843	229	*0.609*	**0.513**

Table 3: Comparison of tracking results for '**many to few**' scenarios with 10% and 25% particle dropout. (AC = # Actual Correspondences, MC = # Measured correspondences, RR = Recovery Ratio, VC = # of Valid Correspondences, MER = Measured error ratio, TER = Total error ratio.)

						Difference of TER Values											
Image Size: 256 x 256						'Few to Many'						'Many to Few'					
Case	Figure	# Vortices	Amplitude	# Particles	Max. Disp.	VSD-TPS	VSD-Labonte	VSD-Baek & Lee	TPS-VSD	TPS-Labonte	TPS-Baek & Lee	VSD-TPS	VSD-Labonte	VSD-Baek & Lee	TPS-VSD	TPS-Labonte	TPS-Baek & Lee
1	-	1	16	200	16	0.00	-0.01	0.01	0.00	-0.01	0.01	-0.01	-0.02	0.04	0.01	0.00	0.05
2	-	1	16	600	16	0.01	0.37	0.02	-0.01	0.36	0.01	0.00	0.39	0.07	0.00	0.38	0.07
3	-	1	32	200	32	0.03	0.24	0.15	-0.03	0.21	0.13	0.02	0.25	0.20	-0.02	0.23	0.18
4	-	1	32	600	32	0.03	0.70	0.31	-0.03	0.67	0.28	-0.05	0.69	0.26	0.05	0.73	0.31
5	-	4	16	200	16	0.01	0.10	0.11	-0.01	0.09	0.10	0.03	0.03	0.11	-0.03	0.00	0.08
6	-	4	16	600	16	0.00	0.68	0.13	0.00	0.68	0.12	-0.02	0.60	0.17	0.02	0.62	0.19
7	-	4	32	200	32	0.00	0.74	0.47	0.00	0.74	0.47	-0.01	0.63	0.38	0.01	0.64	0.39
8	-	8	16	600	16	0.03	0.76	0.28	-0.03	0.73	0.25	0.00	0.60	0.19	0.00	0.60	0.19
9	-	16	16	600	16	0.01	0.72	0.46	-0.01	0.71	0.45	-0.01	0.53	0.32	0.01	0.53	0.33

Table 4: Average difference in the total error ratio (TER) over all particle dropout scenarios for each of the nine test cases presented in tables 2 and 3

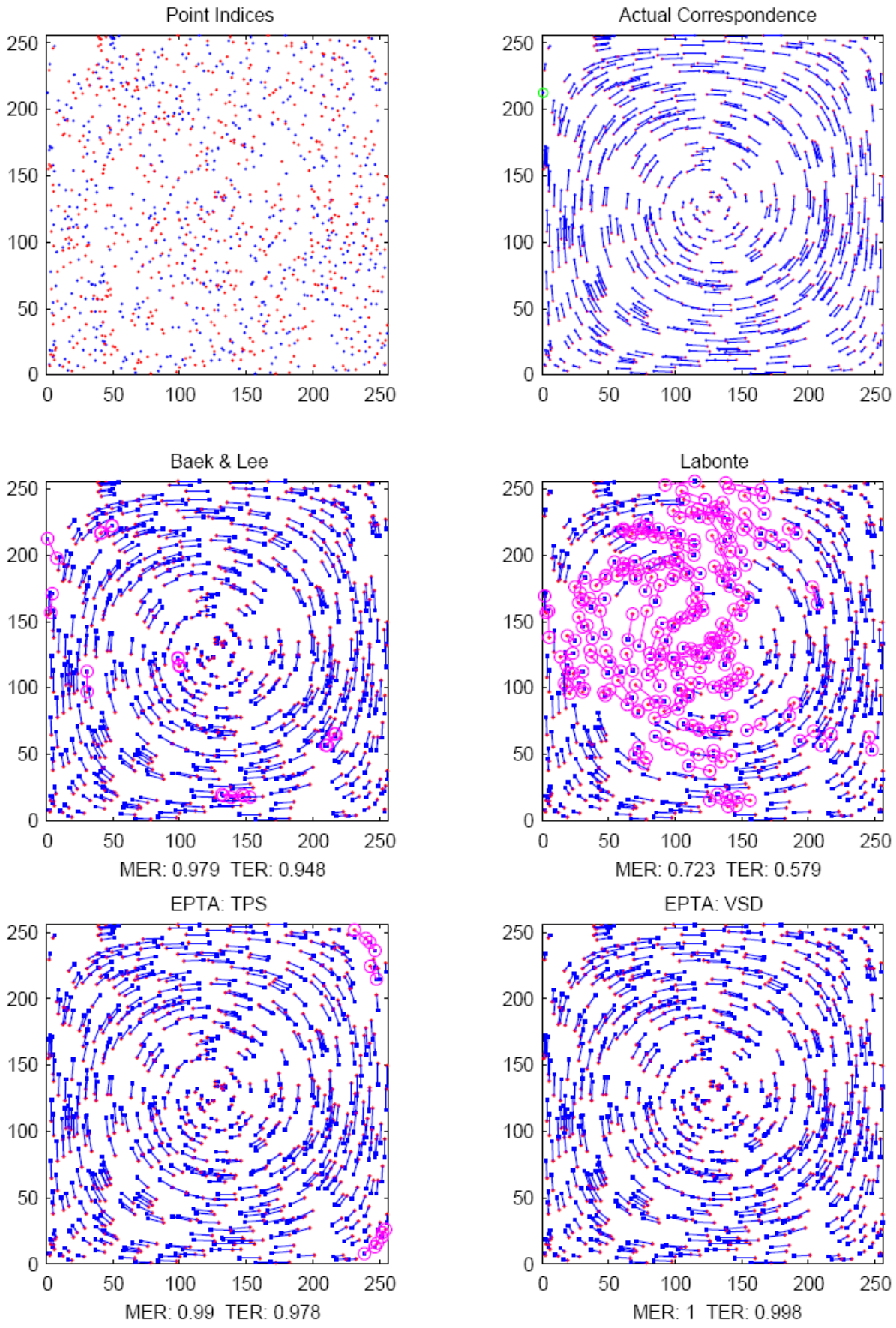

Figure 4: Case 2: 1 Vortex, 600 particles, maximum displacement 16 pix, DR = 3.13, DS = 0.125